

Coherent Control of an Embedded Bound State Without a Spectral Gap

Yue Chang^{1,*}

¹*Beijing Academy of Quantum Information Sciences, Beijing 100193, China*

Bound states in the continuum (BICs) can confine photonic excitations in open systems without conventional cavities or band gaps, making them natural candidates for long-lived quantum storage and single-photon control. Their use is limited, however, by two obstacles: they are dark to incident photons, and they lack spectral-gap protection from the surrounding continuum. We overcome both limitations in a giant atom coupled to a one-dimensional waveguide using two temporal control knobs. Atomic-frequency modulation breaks and restores the destructive-interference condition, enabling deterministic capture and release of mode-matched single photons. Coupling modulation instead preserves the BIC condition while tuning the atomic and photonic weights of the stored state. A key result is that this embedded state can nevertheless be controlled adiabatically despite the absence of a spectral gap, with an intrinsic leakage probability linear in the ramp rate. By separating radiative access from BIC-preserving deformation, the protocol turns a dark BIC into a single-photon memory whose fidelity is set by the intrinsic continuum-induced leakage law, providing a route to embedded-state control in open photonic platforms.

Introduction— Bound states in the continuum (BICs) are localized eigenstates with energies inside a continuum of propagating modes. Their radiative decay is suppressed by symmetry, destructive interference, or parameter tuning. Since the construction of von Neumann and Wigner [1], BICs have become a general wave phenomenon in photonic, acoustic, electronic, and matter-wave systems [2, 3]. In photonics, they enable light confinement in open structures, leading to ultrahigh- Q resonances, enhanced near fields, and narrow spectral features with applications in lasing, nonlinear optics, sensing, wavefront control, and topological photonics [4–10].

For quantum applications, however, the same interference that protects a BIC also creates a control problem. An ideal BIC is dark to the continuum and therefore has vanishing overlap with incoming scattering states. Previous work has shown that initially excited emitters can partially relax into stationary emitter–photon bound states [11, 12], and that a single-excitation BIC can be partly populated through nonlinear multiphoton scattering in waveguide QED [13]. Related waveguide-QED schemes have also used non-Markovian bound states for catch–release protocols, phase-controlled BIC engineering, and BIC-enabled state transfer or entanglement generation [14–16]. These works show that embedded bound states can be accessed and used as quantum channels. They do not, however, address the coherent manipulation of a stored BIC in a genuinely gapless continuum, where no finite spectral separation protects the state from extended scattering modes.

This gapless-control problem is central for using BICs as quantum resources. It is not enough to populate or release a BIC; one must also control its emitter–photon composition during storage. The emitter component provides local addressability for control and readout, whereas the photonic component reduces sensitivity to emitter loss and provides a channel for coupling spatially separated nodes. Dynamically tuning this balance

turns the BIC from a passive embedded state into a controllable quantum memory.

Giant atoms in waveguide quantum electrodynamics (QED) provide a natural setting for this problem. Waveguide QED enables strong and controllable single-photon light–matter interactions in one-dimensional continua [12, 17–26], while giant atoms add spatially separated coupling points whose emitted fields acquire propagation phases and interfere [27–32]. This nonlocal interference gives frequency-dependent decay rates, Lamb shifts, decoherence-free interactions, and non-Markovian multiphoton dynamics [27, 30, 32, 33]. For special propagation phases, destructive interference between radiative channels produces a dressed BIC [11, 13, 34, 35].

In this Letter, we consider a minimal two-point giant atom coupled to a bidirectional one-dimensional waveguide, as shown in Fig. 1(a). We use this model to study two forms of temporal control, illustrated in Fig. 1(b). First, modulating the atomic frequency $\omega(t)$ breaks and restores the BIC condition, thereby coupling the otherwise dark BIC to propagating wavepackets for capture and release. Second, modulating the symmetric atom–waveguide coupling $V(t)$ while maintaining the BIC condition changes the atomic and photonic weights of the stored state without intentionally opening the radiative channel. This second operation realizes adiabatic control without a spectral gap: for a slow coupling ramp, the probability to leave the instantaneous BIC is linear in the ramp rate, rather than quadratically suppressed as in finite-time adiabatic evolution in a gapped system. This scaling originates from the continuum of near-resonant scattering states at the BIC energy. Our work goes beyond static BIC engineering by establishing a dynamical capture–control–release protocol, together with the intrinsic error law for manipulating an embedded photonic quantum state.

Model and BIC— The model setup is shown in Fig. 1.

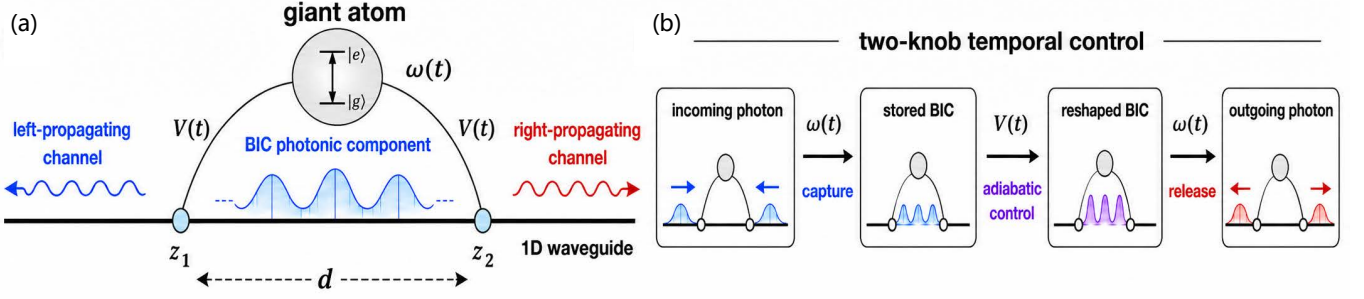


FIG. 1. Two-knob temporal control of a giant-atom BIC. (a) A two-level giant atom couples to a one-dimensional waveguide at two spatially separated points z_1 and z_2 , with separation $d = z_2 - z_1$. For the BIC, the photonic component is confined between the two coupling points. The coupling strength $V(t)$ and the atomic frequency $\omega(t)$ provide independent control knobs. (b) Control protocol. Detuning modulation $\omega(t)$ dynamically breaks and restores the destructive-interference condition, enabling capture of an incoming single-photon wavepacket into the BIC and release into an outgoing photon. Coupling modulation $V(t)$, in contrast, preserves the BIC condition and adiabatically reshapes the stored embedded state by changing its atomic and photonic weights.

Setting the photon velocity to unity, the Hamiltonian is

$$H = \omega \sigma^\dagger \sigma + \int dz \left(i \psi_L^\dagger \partial_z \psi_L - i \psi_R^\dagger \partial_z \psi_R \right) + \sum_{j=1,2} V_j \sigma \left[\psi_L^\dagger(z_j) + \psi_R^\dagger(z_j) \right] + H.c. \quad (1)$$

Here, $\sigma = |g\rangle\langle e|$, ω is the atomic transition frequency, and $\psi_{L(R)}(z)$ is the annihilation operator of the left (right)-propagating waveguide field at point z , V_j is the atom-waveguide coupling constant at the position z_j . In the single-excitation sector, the BIC condition is $V_1 = V_2$ and $\omega d = (2n + 1)\pi$, or $V_1 = -V_2$ and $\omega d = 2n\pi$, where n is an integer. In the following, we focus on the symmetric case $V_1 = V_2 = V$. The energy of the BIC is ω and the state is

$$|B\rangle = \frac{1}{\sqrt{\mathcal{N}}} \left[\sigma^\dagger - iV \int_0^d dz \sum_{\alpha=L,R} m_\alpha e^{im_\alpha \omega z} \psi_\alpha^\dagger(z) \right] |0\rangle, \quad (2)$$

where $|0\rangle$ is the ground states with no atomic or photonic excitation, $m_R = -m_L = 1$, the normalization factor $\mathcal{N} = 1 + 2V^2d$. The BIC therefore contains an atomic component and a photonic component confined between the two coupling points.

Under temporal modulation of $\omega(t)$ and $V(t)$, a general single-excitation state can be written as

$$|\psi(t)\rangle = c_e(t) \sigma^\dagger |0\rangle + \int dz \sum_{\alpha=L,R} u_\alpha(z,t) \psi_\alpha^\dagger(z) |0\rangle, \quad (3)$$

where $c_e(t)$ is the atomic excitation amplitude, $u_\alpha(z,t)$ is the wavefunction of the left- or right-propagating photon at time t and position z . For the symmetric geometry considered here, the field amplitudes satisfy $u_L(z,t) = u_R(d-z,t)$ [36].

Capture and release— The first control knob is the atomic detuning. We keep the coupling V fixed and write $\omega(t) = \omega_0 + \Delta(t)$, where $\omega_0 d = (2n + 1)\pi$ satisfies the BIC condition for the symmetric coupling configuration. For release, the system is initialized in the BIC at $\Delta(0) = 0$, and $\Delta(t) \neq 2n\pi$ is then turned on. In the rotating frame with respect to the frequency ω_0 , $c_e(t) = \tilde{c}_e(t)e^{-i\omega_0 t}$, the exact single-excitation dynamics reduces to the delay equation

$$\partial_t \tilde{c}_e(t) = -i\Delta(t)\tilde{c}_e(t) - 2V^2\tilde{c}_e(t) + 2V^2\tilde{c}_e(t-d), \quad (4)$$

with the BIC history $\tilde{c}_e(t \leq 0) = 1/\sqrt{\mathcal{N}}$. The last term in Eq. (4) describes the field emitted at one coupling point and reabsorbed at the other after the propagation time d . Eq. (4) shows explicitly that detuning does not simply change the phase of the stored excitation: it breaks the delayed destructive interference and converts the BIC into a radiating state. Taking an exponential detuning protocol $\Delta(t) = \Delta_0(1 - e^{-\gamma_\omega t})$, we plot the normalized atomic population $|c_e(t)/c_e(0)|^2$ for different ramp rate γ_ω in Fig. 2(a). As γ_ω increases, the system reaches the radiative detuned regime more rapidly, leading to a faster decay of the atomic population. In contrast, the decay is not a monotonic function of the atom-waveguide coupling strength $\Gamma = 2V^2$, as shown in Fig. 2(b). As Γ increases, the decay first becomes faster and then slows down. The reason is that increasing Γ has two competing effects: it enhances the bare radiative coupling, but it also increases the delayed feedback and makes the BIC more photonic. At large Γ , the state is mostly stored in the photonic component between the coupling points, and delayed feedback dominates over local emission. The trapping effect then wins, and the long-time release becomes slower.

The right-propagating output field $\tilde{u}_R(z,t) = u_R(z,t)e^{i\omega_0(t-z)}$ can be constructed directly from $c_e(t)$

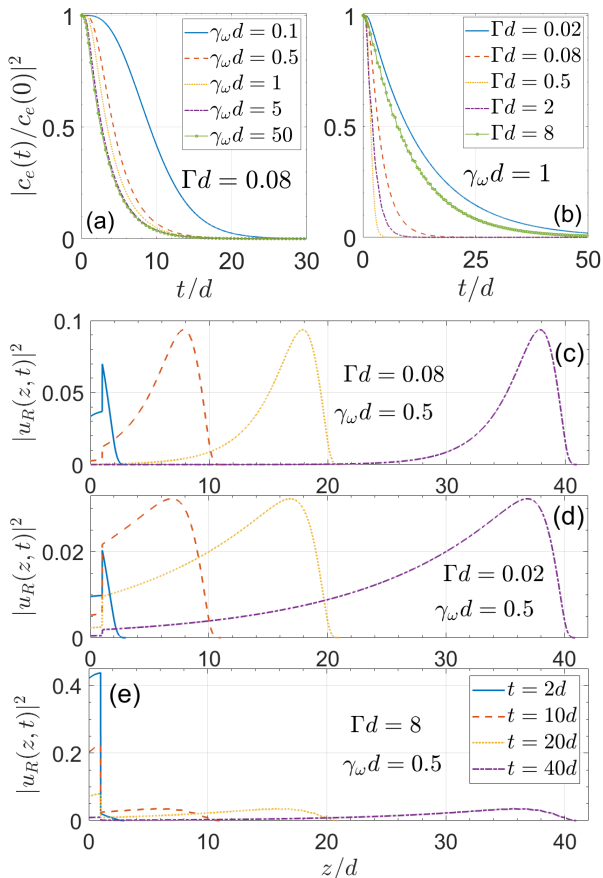


FIG. 2. Release of the BIC by detuning modulation. (a) Decay of the normalized atomic population $|c_e(t)/c_e(0)|^2$ for different detuning ramp rates γ_ω , with fixed atom-waveguide coupling $\Gamma d = 0.08$. (b) Decay of $|c_e(t)/c_e(0)|^2$ for different coupling strengths Γ , with fixed ramp rate $\gamma_\omega d = 1$. The release is nonmonotonic in Γ because stronger coupling enhances both radiative emission and delayed feedback from the confined photonic component. (c)–(e) Right-propagating output intensity $|u_R(z,t)|^2$ at different times, for fixed $\gamma_\omega d = 0.5$ and several values of Γ . At long times, after the stored excitation has been fully emitted into the waveguide, the output field becomes continuous.

as [36]

$$i\tilde{u}_R(z,t) = V\Theta(-\xi)\Theta(\xi+d) + V\tilde{c}_e(\xi)\Theta(\xi)\Theta(z) - V\tilde{c}_e(\xi+d)\Theta(\xi+d)\Theta(z-d). \quad (5)$$

where $\xi = t - z$. Here, on the right-hand side, the first term is the initially trapped BIC field, while the last two terms are the fields emitted from the two coupling points z_1 and z_2 respectively. Since the field is right propagating, $\tilde{u}_R(z,t)$ is nonzero only for $z \in [0, t+d]$. The same nonmonotonic dependence on Γ is visible in the outgoing photonic wavefunctions, as shown in Figs. 2(c)–(e). For $\Gamma d = 0.08$, the photonic excitation leaves the coupling region $z \in [0, d]$ relatively rapidly. By contrast, for either weaker coupling, $\Gamma d = 0.02$, or stronger cou-

pling, $\Gamma d = 8$, the emission is slower. This behavior is consistent with the decay of the atomic excitation. In addition, for finite time $\tilde{u}_R(z,t)$ is discontinuous at $z = 0$ and $z = d$, reflecting the delayed emission from the two coupling points. At long times, after the trapped component has been released, the outgoing wavepacket becomes continuous, as shown in Fig. 2(c).

If a detuning protocol $\Delta(t)$ releases the BIC into an outgoing wavepacket, the time-reversed detuning profile captures the time-reversed wavepacket back into the BIC. This gives a direct route to unit-efficiency loading. In a symmetric two-port geometry, the time-reversed input generally consists of a pair of counterpropagating wavepackets satisfying the same spatial symmetry, $u_L(z,t) = u_R(d-z,t)$. We note that not every incoming wavepacket can be perfectly captured by detuning modulation [36]. Perfect capture requires mode-matched incident wavepacket, which can in principle be generated on demand using a driven three-level emitter in a cavity- or waveguide-QED interface, where the temporal envelope is set by the classical control field [37–41].

Adiabatic control— We now turn to the second control knob, the atom-waveguide coupling. In contrast to detuning modulation, we keep the atomic frequency fixed at the BIC value $\omega(t) = \omega_0$ and modulate the symmetric coupling strength $V(t)$. The destructive-interference condition is then preserved at all times. Therefore, the instantaneous Hamiltonian always has a BIC $|B(t)\rangle$ as its instantaneous eigenstate, with the same form as Eq. (2), but with time-dependent coupling amplitude $V(t)$ and normalization factor $\mathcal{N}(t) = 1 + 2V^2(t)d$. Changing $V(t)$ therefore reshapes the stored BIC without intentionally opening the radiative channel. If the system follows the instantaneous BIC, the atomic and photonic weights are $P_e(t) = 1/[1 + 2V^2(t)d]$ and $P_{\text{ph}}(t) = 2V^2(t)d/[1 + 2V^2(t)d]$, respectively. Thus coupling modulation continuously tunes the BIC between more atom-like and more photon-like configurations: the former is more locally addressable, whereas the latter is better protected from emitter decay or dephasing.

The nontrivial point is that this control is performed without a spectral gap. Although the instantaneous BIC remains an eigenstate throughout the protocol, its energy lies inside the continuum. Thus, the standard gap-based adiabatic argument does not directly apply. To quantify the resulting deformation, we study the full-time dynamics and expand the state in the instantaneous BIC and scattering eigenstates,

$$|\psi(t)\rangle = b(t)|B(t)\rangle + \sum_{\alpha=\pm} \int dk A_{\alpha k}(t)|\psi_{\alpha k}(t)\rangle, \quad (6)$$

where $|\psi_{\alpha k}(t)\rangle$ is the normalized single-photon scattering state with incident momentum k , and $\alpha = \pm$ labels the states with right- and left-propagating incident photons, respectively. Treating the nonadiabatic coupling from

$|B(t)\rangle$ to the scattering continuum perturbatively, the leading scattering amplitude is

$$A_{\alpha k}^{(1)}(t) = - \int_0^t dt' e^{-ik(t-t')} e^{-i\omega_0 t'} \langle \psi_{\alpha k}(t') | \partial_{t'} B(t') \rangle. \quad (7)$$

We note that in the integration, the transition amplitude $\langle \psi_{\alpha k}(t) | \partial_t B(t) \rangle = \langle \psi_{\alpha k}(t) | \partial_t H | B(t) \rangle / (\omega_0 - k)$ is finite as $k \rightarrow \omega_0$. This makes controlled adiabatic deformation possible despite the absence of a gap.

The adiabatic control error is quantified by the leakage probability $P_{\text{leak}} = \sum_{\alpha=\pm} \int dk |A_{\alpha k}(t)|^2$ into the scattering channel. For a slow ramp, the dominant contribution comes from near-resonant scattering states and P_{leak} can be approximated as

$$P_{\text{leak}} \simeq 2d^2 \int dt \frac{\dot{V}^2(t)}{[1 + 2dV^2(t)]^3}. \quad (8)$$

If the ramp rate $\dot{V}(t) \sim \gamma$, Eq. (8) gives $P_{\text{leak}} \propto \gamma$. This linear scaling differs from the usual finite-time gapped adiabatic result, where the leakage probability is generically quadratic in the ramp rate. In a gapped system, every leakage channel has a finite energy mismatch Δ_n , so the phase factor $\exp\left[i \int^t \Delta_n(t') dt'\right]$ oscillates throughout the protocol. Integration by parts then gives a transition amplitude $A_n \sim \gamma$ and hence a probability $P_n \sim \gamma^2$. For the BIC, however, the leakage states form a continuum with detuning $p = k - \omega_0$ that can be arbitrarily small. Modes with $|p| \lesssim \gamma$ do not acquire enough phase to average out during the ramp. The transition amplitude into each such near-resonant mode is set by the total change of the BIC and is not suppressed by an additional gap factor, while the width of the resonant window is $\sim \gamma$. Integrating over these modes therefore gives $P_{\text{leak}} \sim \gamma$. Equivalently, the continuum converts the squared ramp velocity into an instantaneous leakage rate, $\Gamma_{\text{leak}}(t) \sim \dot{V}(t)^2$, and the total probability scales as $\int_0^T dt \dot{V}(t)^2 \sim \gamma$.

For an exponential ramp $V(t) = V_0 + \Delta V(1 - e^{-\gamma_V t})$ from an initial value V_0 to a final value $V_f = V_0 + \Delta V$ with ramp rate γ_V , in Figs. 3(a) and (b) we plot the normalized atomic population $|c_e(t)/c_e(0)|^2$ for different ramp rate γ_V , using the exact delay-differential dynamics

$$\partial_t \tilde{c}_e(t) = -2V^2(t)\tilde{c}_e(t) + 2V(t)V(t-d)\tilde{c}_e(t-d), \quad (9)$$

with the BIC history before the ramp. The adiabatic result

$$\left| \frac{c_e(t)}{c_e(0)} \right|^2 = \frac{1 + 2V_0^2 d}{1 + 2V^2(t) d} \quad (10)$$

is also shown in the figure, which tends to $(1 + 2V_0^2 d) / (1 + 2V_f^2 d)$ for all the ramp rates in the long-term limit. Here, $V_0 \sqrt{d} = 1$ and $\Delta V \sqrt{d} = \pm 0.5$.

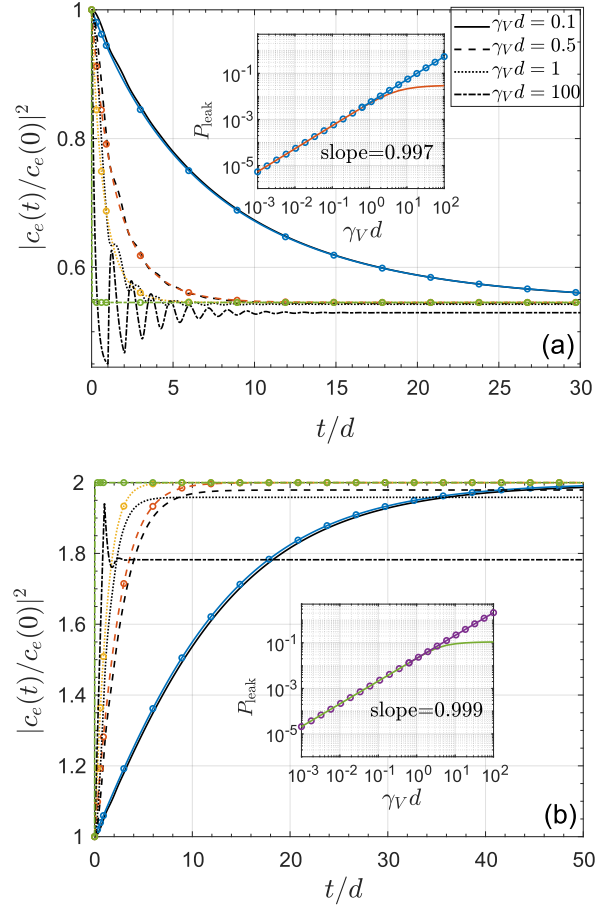


FIG. 3. Adiabatic control of the BIC. (a),(b) Normalized atomic population $|c_e(t)/c_e(0)|^2$ during coupling modulation $V(t) = V_0 + \Delta V(1 - e^{-\gamma_V t})$, for (a) $\Delta V \sqrt{d} = 0.5$ and (b) $\Delta V \sqrt{d} = -0.5$. Solid lines show the exact delay-differential dynamics, while colored dashed lines with open circles show the corresponding instantaneous adiabatic prediction in Eq. 10. For slow ramps, $\gamma_V d \ll 1$, the system follows the instantaneous BIC and the atomic population approaches the adiabatic value. The insets show the leakage probability P_{leak} in the final steady state as a function of the ramp rate γ_V . Solid lines show the leakage extracted from the exact delay-differential dynamics; fits for $\gamma_V d < 0.5$ give slopes close to unity, confirming $P_{\text{leak}} \propto \gamma_V$. Lines with circles show the perturbative prediction of Eq. 8, which agrees with the exact result for small $\gamma_V d$.

We see from the figures that the system adiabatically follows the instantaneous BIC for $\gamma_V d \ll 1$, demonstrating high-fidelity coherent control between an atom-like state and a photon-like state.

The exact leakage is obtained from the emitted field outside the interval $[0, d]$, with the wavefunction determined by $\tilde{c}_e(t)$ as

$$i\tilde{u}_R(z, t) = V_0 \Theta(-\xi) \Theta(\xi + d) + V(\xi) \tilde{c}_e(\xi) \Theta(\xi) \Theta(z) - V(\xi + d) \tilde{c}_e(\xi + d) \Theta(\xi + d) \Theta(z - d). \quad (11)$$

The insets of Figs. 3(a) and 3(b) compare the exact leak-

age extracted from the exact delay equation with the perturbative prediction of Eq. (8) as a function of $\gamma_V d$. The two results agree and both show the linear scaling $P_{\text{leak}} \propto \gamma_V$ in the slow-ramp regime. By contrast, in the sudden-ramp limit the leakage is set by the overlap error between the initial and final BICs. [36]

$$P_{\text{leak}} = 1 - \frac{(1 + 2V_0 V_f d)^2}{(1 + 2V_0^2 d)(1 + 2V_f^2 d)}. \quad (12)$$

This is consistent with the saturation values indicated in Figs. 3(a) and (b).

Conclusion and outlook— We have studied the dynamical control of a bound state in the continuum (BIC) in a giant-atom waveguide-QED system. The two control knobs address the two basic obstacles to using a BIC as a quantum resource. Detuning modulation breaks and restores the destructive-interference condition, thereby coupling the otherwise dark state to propagating wavepackets and providing a capture–release interface. Symmetric coupling modulation, instead, preserves the BIC condition and changes the atom–photon composition of the stored state without intentionally opening a radiative channel. The latter operation realizes adiabatic control in the absence of a spectral gap. Because the BIC remains embedded in the scattering continuum, the leakage is not governed by the usual gapped adiabatic scaling. We derived the leading leakage probability and found $P_{\text{leak}} \propto \gamma$ for an exponential ramp with rate γ . This linear scaling arises from near-resonant scattering states at the BIC energy and is confirmed by exact delay-differential dynamics.

These results establish a coherent capture–control–release protocol for a giant-atom BIC, together with the intrinsic error law for manipulating an embedded photonic state. More broadly, the separation of radiative access from BIC-preserving deformation may provide a useful principle for dynamical BIC control in other open quantum systems. Possible extensions include chiral or asymmetric giant-atom geometries for directional capture and release, multi-giant-atom networks for distributed storage and BIC-mediated entanglement generation, and optimized ramp protocols that reduce continuum-induced leakage relative to the simple adiabatic ramps considered here.

Acknowledgment— This work was supported by the National Natural Science Foundation of China under Grant No. 12575008.

* yuechang7@gmail.com

[1] J. von Neumann and E. Wigner. Über merkwürdige diskrete eigenwerte. *Physikalische Zeitschrift*, 30:465–467, 1929. URL https://link.springer.com/chapter/10.1007/978-3-662-02781-3_19.

- [2] Chia Wei Hsu, Bo Zhen, A. Douglas Stone, John D. Joannopoulos, and Marin Soljačić. Bound states in the continuum. *Nature Reviews Materials*, 1:16048, 2016. doi:10.1038/natrevmats.2016.48. URL <https://doi.org/10.1038/natrevmats.2016.48>.
- [3] Almas F. Sadreev. Interference traps waves in an open system: bound states in the continuum. *Reports on Progress in Physics*, 84:055901, 2021. doi:10.1088/1361-6633/abefb9. URL <https://doi.org/10.1088/1361-6633/abefb9>.
- [4] Chia Wei Hsu, Bo Zhen, Jeongwon Lee, Song-Liang Chua, Steven G. Johnson, John D. Joannopoulos, and Marin Soljačić. Observation of trapped light within the radiation continuum. *Nature*, 499:188–191, 2013. doi:10.1038/nature12289. URL <https://doi.org/10.1038/nature12289>.
- [5] Bo Zhen, Chia Wei Hsu, Ling Lu, A. Douglas Stone, and Marin Soljačić. Topological nature of optical bound states in the continuum. *Physical Review Letters*, 113:257401, 2014. doi:10.1103/PhysRevLett.113.257401. URL <https://doi.org/10.1103/PhysRevLett.113.257401>.
- [6] Jae Woong Yoon, Seok Ho Song, and Robert Magnusson. Critical field enhancement of asymptotic optical bound states in the continuum. *Scientific Reports*, 5:18301, 2015. doi:10.1038/srep18301. URL <https://doi.org/10.1038/srep18301>.
- [7] Kirill Koshelev, Sergey Lepeshov, Mingkai Liu, Andrey Bogdanov, and Yuri Kivshar. Asymmetric metasurfaces with high- q resonances governed by bound states in the continuum. *Physical Review Letters*, 121:193903, 2018. doi:10.1103/PhysRevLett.121.193903. URL <https://doi.org/10.1103/PhysRevLett.121.193903>.
- [8] Meng Kang, Tao Liu, C. T. Chan, and Meng Xiao. Applications of bound states in the continuum in photonics. *Nature Reviews Physics*, 5:659–678, 2023. doi:10.1038/s42254-023-00642-8. URL <https://doi.org/10.1038/s42254-023-00642-8>.
- [9] Ashok Kodigala, Thomas Lepetit, Qing Gu, Babak Bahari, Yeshiahu Fainman, and Boubacar Kanté. Lasing action from photonic bound states in continuum. *Nature*, 541(7636):196–199, 2017. doi:10.1038/nature20799. URL <https://doi.org/10.1038/nature20799>.
- [10] M. Luo, Y. Zhou, X. Zhao, Z. Guo, Y. Li, Q. Wang, J. Liu, W. Luo, Y. Shi, A. Q. Liu, and X. Wu. High-sensitivity optical sensors empowered by quasi-bound states in the continuum in a hybrid metal-dielectric metasurface. *ACS Nano*, 18(8):6477–6486, 2024. doi:10.1021/acsnano.3c11994. URL <https://doi.org/10.1021/acsnano.3c11994>.
- [11] T. Tufarelli, F. Ciccarello, and M. S. Kim. Dynamics of spontaneous emission in a single-end photonic waveguide. *Physical Review A*, 87:013820, 2013. doi:10.1103/PhysRevA.87.013820. URL <https://doi.org/10.1103/PhysRevA.87.013820>.
- [12] Paolo Facchi, M. S. Kim, Saverio Pascazio, Francesco V. Pepe, Domenico Pomarico, and Tommaso Tufarelli. Bound states and entanglement generation in waveguide quantum electrodynamics. *Physical Review A*, 94:043839, 2016. doi:10.1103/PhysRevA.94.043839. URL <https://doi.org/10.1103/PhysRevA.94.043839>.
- [13] Giuseppe Calajó, Yao-Lung L. Fang, Harold U. Baranger, and Francesco Ciccarello. Exciting a bound state in the continuum through multiphoton scattering plus delayed

- quantum feedback. *Physical Review Letters*, 122:073601, 2019. doi:10.1103/PhysRevLett.122.073601. URL <https://doi.org/10.1103/PhysRevLett.122.073601>.
- [14] Luting Xu and Lingzhen Guo. Catch and release of propagating bosonic field with non-Markovian giant atom. *New Journal of Physics*, 26:013025, 2024. doi:10.1088/1367-2630/ad18ed.
- [15] Xiaojun Zhang, Mingjie Zhu, and Zhihai Wang. Phase-controlled bound states in giant atom waveguide QED setup. *Communications in Theoretical Physics*, 77(11):115102, 2025. doi:10.1088/1572-9494/addb2a.
- [16] Xiang Guo, Xiaojun Zhang, Mingzhu Weng, Qian Bin, Hao-di Liu, Hai-Jun Xing, Xin-You Lü, and Zhihai Wang. Bound state in the continuum and multiple atom state transfer applications in a waveguide QED setup, 2025. arXiv:2512.06365 [quant-ph].
- [17] Jung-Tsung Shen and Shanhui Fan. Strongly correlated two-photon transport in a one-dimensional waveguide coupled to a two-level system. *Physical Review Letters*, 98:153003, 2007. doi:10.1103/PhysRevLett.98.153003. URL <https://doi.org/10.1103/PhysRevLett.98.153003>.
- [18] Tao Shi, Darrick E. Chang, and J. Ignacio Cirac. Multiphoton-scattering theory and generalized master equations. *Physical Review A*, 92:053834, 2015. doi:10.1103/PhysRevA.92.053834. URL <https://doi.org/10.1103/PhysRevA.92.053834>.
- [19] D. Roy, C. M. Wilson, and O. Firstenberg. Colloquium: Strongly interacting photons in one-dimensional continuum. *Reviews of Modern Physics*, 89:021001, 2017. doi:10.1103/RevModPhys.89.021001. URL <https://doi.org/10.1103/RevModPhys.89.021001>.
- [20] X. Gu, A. F. Kockum, A. Miranowicz, Y.-x. Liu, and F. Nori. Microwave photonics with superconducting quantum circuits. *Physics Reports*, 718–719:1–102, 2017. doi:10.1016/j.physrep.2017.10.002. URL <https://doi.org/10.1016/j.physrep.2017.10.002>.
- [21] A. S. Sheremet, M. I. Petrov, I. V. Iorsh, A. V. Poshakinskiy, and A. N. Poddubny. Waveguide quantum electrodynamics: Collective radiance and photon-photon correlations. *Reviews of Modern Physics*, 95:015002, 2023. doi:10.1103/RevModPhys.95.015002. URL <https://doi.org/10.1103/RevModPhys.95.015002>.
- [22] Yue Chang, Alejandro González-Tudela, Carlos Sánchez Muñoz, Carlos Navarrete-Benlloch, and Tao Shi. Deterministic down-converter and continuous photon-pair source within the bad-cavity limit. *Physical Review Letters*, 117:203602, 2016. doi:10.1103/PhysRevLett.117.203602. URL <https://doi.org/10.1103/PhysRevLett.117.203602>.
- [23] Li-Ping Yang and Yue Chang. Quantum beam splitter as a controller of higher-order quantum coherence. *Physical Review A*, 110:023722, 2024. doi:10.1103/PhysRevA.110.023722. URL <https://doi.org/10.1103/PhysRevA.110.023722>.
- [24] Maximilian Zanner, Tuure Orell, Christian M. F. Schneider, Romain Albert, Stefan Oleschko, Mathieu L. Juan, Matti Silveri, and Gerhard Kirchmair. Coherent control of a multi-qubit dark state in waveguide quantum electrodynamics. *Nature Physics*, 18:538–543, 2022. doi:10.1038/s41567-022-01527-w. URL <https://doi.org/10.1038/s41567-022-01527-w>.
- [25] Tao Shi, Ying-Hai Wu, Alejandro González-Tudela, and J. Ignacio Cirac. Bound states in boson impurity models. *Physical Review X*, 6:021027, 2016. doi:10.1103/PhysRevX.6.021027. URL <https://doi.org/10.1103/PhysRevX.6.021027>.
- [26] Tao Shi, Yue Chang, and Juan José García-Ripoll. Ultrastrong coupling few-photon scattering theory. *Physical Review Letters*, 120:153602, 2018. doi:10.1103/PhysRevLett.120.153602. URL <https://doi.org/10.1103/PhysRevLett.120.153602>.
- [27] A. F. Kockum, P. Delsing, and G. Johansson. Designing frequency-dependent relaxation rates and Lamb shifts for a giant artificial atom. *Physical Review A*, 90:013837, 2014. doi:10.1103/PhysRevA.90.013837. URL <https://doi.org/10.1103/PhysRevA.90.013837>.
- [28] M. V. Gustafsson, T. Aref, A. F. Kockum, M. K. Ekström, G. Johansson, and P. Delsing. Propagating phonons coupled to an artificial atom. *Science*, 346:207–211, 2014. doi:10.1126/science.1257219. URL <https://doi.org/10.1126/science.1257219>.
- [29] L. Guo, A. L. Grimsmo, A. F. Kockum, M. Pletyukhov, and G. Johansson. Giant acoustic atom: A single quantum system with a deterministic time delay. *Physical Review A*, 95:053821, 2017. doi:10.1103/PhysRevA.95.053821. URL <https://doi.org/10.1103/PhysRevA.95.053821>.
- [30] A. F. Kockum, G. Johansson, and F. Nori. Decoherence-free interaction between giant atoms in waveguide quantum electrodynamics. *Physical Review Letters*, 120:140404, 2018. doi:10.1103/PhysRevLett.120.140404. URL <https://doi.org/10.1103/PhysRevLett.120.140404>.
- [31] B. Kannan, M. J. Ruckriegel, D. L. Campbell, A. F. Kockum, J. Braumüller, D. K. Kim, M. Kjaergaard, P. Krantz, A. Melville, B. M. Niedzielski, A. Vepsäläinen, R. Winik, J. L. Yoder, F. Nori, T. P. Orlando, S. Gustavsson, and W. D. Oliver. Waveguide quantum electrodynamics with superconducting artificial giant atoms. *Nature*, 583:775–779, 2020. doi:10.1038/s41586-020-2529-9. URL <https://doi.org/10.1038/s41586-020-2529-9>.
- [32] Anton Frisk Kockum. Quantum optics with giant atoms—the first five years. In *International Symposium on Mathematics, Quantum Theory, and Cryptography*, volume 33 of *Mathematics for Industry*, pages 125–146. Springer, Singapore, 2021. doi:10.1007/978-981-15-5191-8_12. URL https://doi.org/10.1007/978-981-15-5191-8_12.
- [33] Yue Chang. Non-Markovian multiphoton chiral dynamics with giant systems. *Communications Physics*, 8:385, 2025. doi:10.1038/s42005-025-02293-w. URL <https://doi.org/10.1038/s42005-025-02293-w>.
- [34] C. González-Ballester, F. J. García-Vidal, and E. Moreno. Non-Markovian effects in waveguide-mediated entanglement. *New Journal of Physics*, 15:073015, 2013. doi:10.1088/1367-2630/15/7/073015. URL <https://doi.org/10.1088/1367-2630/15/7/073015>.
- [35] Xin Wang, Tao Liu, Anton Frisk Kockum, Hui-Ran Li, and Franco Nori. Tunable chiral bound states with giant atoms. *Physical Review Letters*, 126:043602, 2021. doi:10.1103/PhysRevLett.126.043602. URL <https://doi.org/10.1103/PhysRevLett.126.043602>.
- [36] Supplemental material for “coherent control of an embedded bound state without a spectral gap”, 2026. See Supplemental Material for derivations of the delay-differential equations for the atomic excitation and photonic wavefunctions, the scattering states, and the adia-

- batic leakage.
- [37] J. I. Cirac, P. Zoller, H. J. Kimble, and H. Mabuchi. Quantum state transfer and entanglement distribution among distant nodes in a quantum network. *Physical Review Letters*, 78:3221–3224, 1997. doi: 10.1103/PhysRevLett.78.3221. URL <https://doi.org/10.1103/PhysRevLett.78.3221>.
- [38] Matthias Keller, Birgit Lange, Kazuhiro Hayasaka, Wolfgang Lange, and Herbert Walther. Continuous generation of single photons with controlled waveform in an ion-trap cavity system. *Nature*, 431:1075–1078, 2004. doi: 10.1038/nature02961. URL <https://doi.org/10.1038/nature02961>.
- [39] Jerome Dilley, Peter Nisbet-Jones, Bruce W. Shore, and Axel Kuhn. Single-photon absorption in coupled atom-cavity systems. *Physical Review A*, 85:023834, 2012. doi: 10.1103/PhysRevA.85.023834. URL <https://doi.org/10.1103/PhysRevA.85.023834>.
- [40] H. Z. Shen, Y. Chen, T. Z. Luan, and X. X. Yi. Multiple single-photon generations in three-level atoms coupled to a cavity with non-markovian effects. *Physical Review A*, 107:053705, 2023. doi:10.1103/PhysRevA.107.053705. URL <https://doi.org/10.1103/PhysRevA.107.053705>.
- [41] Magdalena Stobińska, Gernot Alber, and Gerd Leuchs. Perfect excitation of a matter qubit by a single photon in free space. *EPL*, 86:14007, 2009. doi: 10.1209/0295-5075/86/14007. URL <https://doi.org/10.1209/0295-5075/86/14007>.